Carbohydrate Polymers 125 (2015) 360–366

Contents lists available at ScienceDirect

Carbohydrate Polymers

journal homepage: www.elsevier.com/locate/carbpol

Extraction of cellulose nano-crystals from old corrugated container fiber using phosphoric acid and enzymatic hydrolysis followed by sonication

Yanjun Tang[a,b,*], Xiaochuang Shen[a], Junhua Zhang[b], Daliang Guo[b], Fangong Kong[c], Nan Zhang[d]

[a] National Engineering Laboratory of Textile Fiber Materials and Processing Technology, Zhejiang Sci-Tech University, Hangzhou 310018, China
[b] Engineering Research Center for Eco-Dyeing & Finishing of Textiles, Ministry of Education, Zhejiang Sci-Tech University, Hangzhou 310018, China
[c] Key Laboratory of Pulp and Paper Science & Technology of Ministry of Education, Qilu University of Technology, Jinan 250353, China
[d] Shanghai Tonnor Material Science Co., Ltd., Shanghai 200092, China

ARTICLE INFO

Article history:
Received 5 January 2015
Received in revised form 25 February 2015
Accepted 27 February 2015
Available online 6 March 2015

Keywords:
Old corrugated container (OCC)
Cellulose nano-crystals (CNC)
Phosphoric acid hydrolysis
Enzymatic hydrolysis
Sonication

ABSTRACT

Due to its amazing physicochemical properties and high environmental compatibility, cellulose nano-crystals (CNC) hold great promise for serving as a strategic platform for sustainable development. Now, there has been growing interest in the development of processes using waste or residual biomass as CNC source for addressing economic and environmental concerns. In the present work, a combined process involving phosphoric acid hydrolysis, enzymatic hydrolysis and sonication was proposed aiming to efficiently exact CNC from low-cost old corrugated container (OCC) pulp fiber. The effect of enzymatic hydrolysis on the yield and microstructure of resulting CNC was highlighted. Results showed that the enzymatic hydrolysis was effective in enhancing CNC yield after phosphoric acid hydrolysis. CNC was obtained with a yield of 23.98 wt% via the combined process with phosphoric acid concentration of 60 wt%, cellulase dosage of 2 mL (84 EGU) per 2 g fiber and sonication intensity of 200 W. Moreover, the presence of enzymatic hydrolysis imparted the obtained CNC with improved dispersion, increased crystallinity and thermal stability.

1. Introduction

Cellulose nano-crystals (CNC), derived from naturally occurring cellulose, has shown great promise in many application fields due to its several key features, *e.g.*, high strength, electro-magnetic response and a large surface area (Cha, He, & Ni, 2012; Sun, Hou, He, Liu, & Ni, 2014; Zaman, Liu, Xiao, Chibante, & Ni, 2013). Currently, CNC may be mainly extracted from forest biomass, such as wood (Beck-Candanedo, Roman, & Gray, 2005; Li, Wang, & Liu, 2011), straw (Tibolla, Pelissari, & Menegalli, 2014; Xu et al., 2013) and cotton fibers (Li, Li, Zou, Zhou, & Lian, 2014; Xiong, Zhang, Tian, Zhou, & Lu, 2012). Despite the abundant availability of raw materials, the development of processes using waste or residual biomass as CNC source is of practical interest (Brinchi, Cotana, Fortunati, & Kenny, 2013). Old corrugated container (OCC) fiber, a high volume, low-cost recycled feedstock, currently, is mainly used to cost-effectively produce new paper for new board and new containers (Hunter & Park, 1998; Nguyen, Shariff, Earl, & Eamer, 1993). OCC is mainly composed of cellulose, with low content of hemicellulose, lignin and impurities (Wan, Yang, Ma, & Wang, 2011), and therefore has the potential to be used as alternative raw material for CNC production. However, there has been limited study regarding the production of CNC using OCC fiber as raw materials in the literature. In this sense, an attempt to investigate the possibility and feasibility of efficiently extracting CNC from OCC fiber would provide an opportunity to find a potential source candidate for the cost-effective production of CNC.

In the production of CNC, sulfuric acid hydrolysis is one of the most commonly used processes (Bai, Holbery, & Li, 2009; Xiong et al., 2012). However, the use of sulfuric acid has a number of important drawbacks. One major drawback is that the sulfate groups introduced to the CNC via sulfuric acid hydrolysis catalyze the degradation of cellulose, particularly at higher temperature (Camarero Espinosa, Kuhnt, Foster, & Weder, 2013), which resulted

* Corresponding author at: National Engineering Laboratory of Textile Fiber Materials and Processing Technology, Zhejiang Sci-Tech University, Hangzhou 310018, China. Tel.: +86 57186843561.
E-mail address: tangyj@zstu.edu.cn (Y. Tang).

http://dx.doi.org/10.1016/j.carbpol.2015.02.063
0144-8617/

in the limited thermal stability, thus exerting a negative effect on the potential application of CNC in nanocomposites (Filson & Dawson-Andoh, 2009; Li, Yue, & Liu, 2012). For this reason, an increasing effort was made to the use of mineral acids other than sulfuric acid for the hydrolysis of cellulose in recent years (Camarero Espinosa et al., 2013; Liu et al., 2014; Yu et al., 2013). Among these mineral acids, phosphoric acid has shown its potential to be a promising alternative to sulfuric acid for cellulose hydrolysis on account of the enhanced thermal stability and biocompatibility of the produced CNC (Camarero Espinosa et al., 2013; Li et al., 2013). Apart from acid hydrolysis, some eco-friendly approaches, *e.g.*, high-intensity sonication (Li et al., 2011, 2012) and enzymatic hydrolysis (Pirani & Hashaikeh, 2013) have been developed in the past decades for CNC production. For instance, Chen (Chen et al., 2011) examined the individualization of cellulose nanofibers from poplar wood using chemical pretreatment and high-intensity sonication, and found that the diameter distributions of the resulting nanofibers were dependent on the output power of the ultrasonic treatment. de Campos (de Campos et al., 2013) also obtained nanofibers from sugarcane bagasse fiber using enzymatic hydrolysis followed by sonication. Lu (Lu, Gui, Zheng, & Liu, 2013) proposed the method of sulfuric acid hydrolysis accompanied with sonication and homogenization for isolating nanofibers from sweet potato residue. However, no information was provided with regard to the yield of produced nanofibers in each of the above cases. In general, CNC may be currently produced from different cellulosic materials using various processes. CNC yield, however, one key factor affecting the production efficiency, may vary widely, depending on the source of cellulosic materials and the applied process. Efforts in increasing the yield in CNC extraction play an important role in final cost. In this regard, the improvement of separation technologies and development of combined processes could be one of the most effective ways to address the yield limitation issue. In fact, in our previous work (Tang, Yang, Zhang, & Zhang, 2014), a low-intensity sonication concept was proposed to improve the yield of CNC based on sulfuric acid hydrolysis. The results demonstrated that the overall yield of CNC was increased from 33.0% to 40.4% as a result of the supplement of sonication at 100 W for 30 min compared to the conventional sulfuric acid hydrolysis.

The present paper described the isolation of CNC from OCC. We aimed to maximize the yield of CNC by using a combined process consisting of phosphoric acid hydrolysis, enzymatic hydrolysis and sonication. The dominant role of enzymatic hydrolysis in enhancing CNC yield, a key factor determining the economics of the provided process, was highlighted by varying the time of enzymatic hydrolysis. Furthermore, the characterization of CNC samples was carried out by using TEM, FT-IR, XRD, TGA, particle size distribution determination and rheological measurements. The study would be helpful in assessing the feasibility of isolating CNC from OCC and its potential as a reinforcing component in nanocomposite application.

2. Experimental

2.1. Materials

Old corrugated container (OCC) material was received from a paper mill in Eastern China. Cellulase (Celluclast 1.5 L FG possessing activity of 700 EGU/g) was supplied by Novozymes Investment Co. Ltd. Sodium hydroxide (NaOH) and anhydrous ethanol were purchased from Hangzhou Gao Jing fine Chemical Instrument Co., Ltd., China. Dimethyl sulfoxide and phosphoric acid (H_3PO_4) were purchased from Tianjin Branch Close the Chemical Reagent Co., Ltd., China. Distilled water was used for all experiments.

2.2. Preparation of CNC

2.2.1. Mechanical pretreatment

500 g of OCC (based on dry weight) was torn into pieces of 5 × 5 cm and soaked in 4500 mL of distilled water for 24 h at room temperature before mechanical agitation for 10 min to release fibers. This mixture was then pulped for 15 min at room temperature using an N-196VT pulper from Adirondack Machine Corp.

2.2.2. Sodium hydroxide pretreatment

100 g of treated OCC pulp fiber (based on dry weight) was dispersed into 1000 mL of NaOH solution (1.0 wt%) and kept stirring for 3 h at 60 °C. The chemically pretreated pulp was then subjected to conventional washing and screening (ZQS15) operations for the purpose of removing impurities from OCC pulp. Afterwards, the pulp fiber suspension was centrifuged at 5000 rpm for 10 min, and the supernatant fluid was decanted to remove NaOH. The washing procedure was repeated several times until the pH of solution was 7.

2.2.3. Phosphoric acid hydrolysis

20 g of above treated fiber (based on dry weight) was dissolved in 250 mL of 60% (w/w) H_3PO_4 solution. The reaction was performed in a water bath under stirring for 6 h at room temperature. Then 150 mL of 25% (w/w) dimethyl sulfoxide was added, which made cellulosic fiber precipitate immediately. After that, the suspension was centrifuged at 5000 rpm for 10 min at room temperature, and the supernatant fluid was decanted to remove H_3PO_4 and dimethyl sulfoxide. The washing procedure was also repeated several times until the pH of solution was 7.

2.2.4. Enzymatic hydrolysis

Initially, 2 g of the fiber obtained from phosphoric acid hydrolysis was dispersed (GFJ-04, Shanghai modern environmental technology Co., Ltd., China.) into 250 mL of distilled water in a 500 mL flask. Secondly, the mixture was further dispersed (RW20 digital, IKA, Germany) for 2 h at 200 rpm and 50 °C. Afterwards, 2 mL of cellulase enzyme (84 EGU) was added into the resulting mixture and reacted for 1 (or 12, 24, 36) h at 50 °C. After the reaction was run for a desired duration, 25 mL of anhydrous ethanol was added to terminate the action of cellulose (Filson, Dawson-Andoh, & Schwegler-Berry, 2009).

2.2.5. Ultrasonic treatment

The resulting suspension subsequently underwent ultrasonic treatment (JY92-IIDN, Ningbo Xingzhi Biotechnology Co., Ltd., China.) for 10 min at 200 W for further enhancing the CNC extraction yield. Then the suspension was centrifuged at 11,000 rpm for 10 min at 25 °C and the supernatant fluid was decanted to remove cellulase. This process was repeated for 5–6 times until the supernatant fluid turned turbid. The turbid liquid was collected that contained the release of the nanocrystals cellulose. The process was continuously repeated until the turbid liquid became clear. The total turbid solution collected for each treatment was filtered with distilled water in a dialysis bag. Eventually, the above suspension was dried in an oven at 80 °C until the moisture content was reduced about 50%, followed by freeze-drying (LGJ-10, Beijing Source Huaxing Technology Development Co., Ltd., China.), prior to the subsequent characterization.

2.3. Analysis and characterization

2.3.1. CNC yield calculation

CNC yield (%) was calculated using the following equation:

$$Yield\ (\%) = \frac{(M_2 - M_3) \times V_1}{M_1 \times V_2} \times 100\% \quad (1)$$

In Eq. (1), M_1 represents the mass of pulp fiber after sodium hydroxide pre-treatment, M_2 denotes the total mass of oven-dried CNC and bottle, M_3 is the mass of the bottle, V_1 is the total volume of prepared CNC suspension, and V_2 is the volume of CNC suspension for oven-drying.

2.3.2. Particle size distribution determination

The dried CNC samples were re-dispersed in distilled water to achieve a concentration of 1.0 wt%, and then sonicated using an ultrasonic processor (200 W, 120 s). The measurement of particle size distribution and average particle size of CNC samples was conducted using LB-550 type particle size analyzer (Horiba, Japan).

2.3.3. Rheological measurements

The rheological measurements involving viscosity, complex viscosity and storage modulus of CNC suspensions with a solid content of 0.4 wt% were conducted on a cylinder rotary rheometer (Physica MCR301, Anton Paar, Austria). Measurements were acquired for all samples at 25 °C.

2.3.4. Transmission electron microscopy observations

CNC coated grids were examined using a transmission electron microscopy (TEM) (JEOL, Japan) at an operating voltage of 80 kV. A drop of CNC suspension was deposited on carbon-coated grids and allowed to dry at room temperature.

2.3.5. Fourier-transformed infrared spectra analysis

Fourier-transformed infrared (FT-IR) spectra of CNC samples were collected using a Nicolet 5700 FT-IR spectrometer in the wavenumber range between 4000 and 500 cm^{-1}, at a spectral resolution of 4 cm^{-1}. Each sample was palletized with KBr powder to prepare pastille.

2.3.6. X-ray diffraction analysis

The X-ray diffraction (XRD) patterns for all CNC samples were characterized with an X-ray diffractometer (X'TRA-055, ARL, Switzerland) using a Cu Kα radiation (λ = 0.154 nm) at 50 kV and 100 mA. Scattered radiation was detected in the range of 2θ = 10–50°, at a scan rate of 2 °/min. Based on XRD data, the Segal crystalline index (CI) of CNC samples was calculated following the method described in an earlier work (French & Cintrón, 2013).

2.3.7. Thermo gravimetric analysis

Thermo gravimetric analysis (TGA) (Perkin Elmer, USA) was carried out under atmosphere nitrogen. The weight of the samples was varied from 6 to 8 mg. The temperature was increased from 50 °C to 700 °C at a heating rate of 20 °C/min.

3. Results and discussion

3.1. Proposed process for CNC production from OCC

Scheme 1 shows a simplified process flow diagram related to the integrated processing of OCC for the isolation of CNC. Overall, OCC pulp fiber consists of plenty of cellulose, a small quantity of hemicelluloses, lignin and impurities (Guo, Wang, Wan, & Ma, 2011), which make it a feasible option as a raw material for CNC production. To improve the accessibility and reactivity of OCC pulp fiber, it is rather essential to create more accessible sites by mechanical and/or chemical pretreatment prior to the tailored hydrolysis (Engström, Ek, & Henriksson, 2006). In this regard, OCC here was first soaked in distilled water, agitated to release fibers and then pulped in a pulper followed by an alkaline pretreatment process for improving the subsequent hydrolysis efficiency.

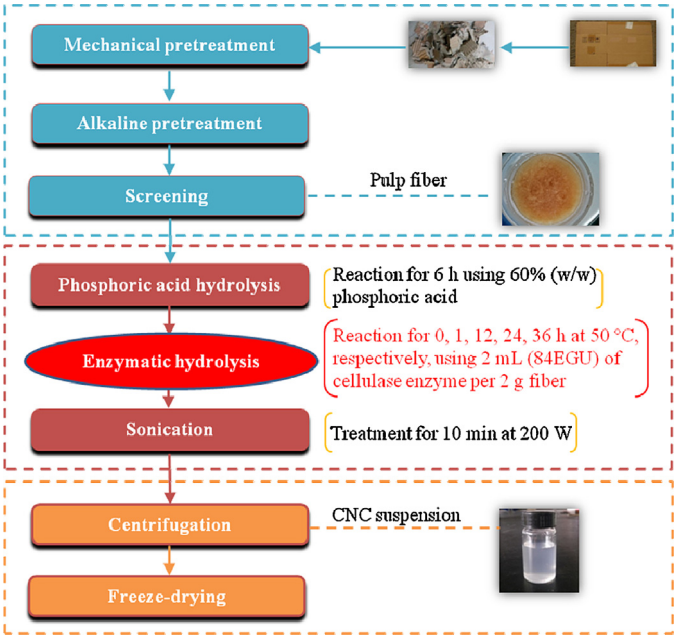

Scheme 1. Proposed process for CNC production from OCC.

Native cellulose consists of amorphous and crystalline regions, and the amorphous regions have lower density compared to the crystalline regions. Thus, when cellulose fibers were subjected to harsh acid treatment, the amorphous regions break up, releasing the individual crystallites (Flauzino Neto, Silvério, Dantas, & Pasquini, 2013). Besides, it is widely accepted that enzymatic treatment and/or sonication may be promising approaches for the enhancement of CNC yield. It should be noted that sonication is non-selective, implying that both the crystalline and amorphous area of cellulose can be removed, thus leading to the decreased crystallinity of the NCC, which had been greatly identified in the previous work (Li et al., 2012). On the other hand, the sonication impact can break the relatively weak interfaces among the nanofibers, gradually disintegrating the microsized cellulose fibers into nanofibers (Tischer, Sierakowski, Westfahl, & Tischer, 2010), which could facilitate the CNC production. As a result, sonication was often used for assisting the production of CNC. Herein, a combined process involving phosphoric acid hydrolysis, enzymatic hydrolysis and sonication was developed for efficiently isolating CNC from OCC fiber. In particular, the role of the enzymatic hydrolysis in improving the CNC yield after phosphoric acid hydrolysis was highlighted. In principle, enzymatic treatment would further lead to increased porosity/openness of cellulose, resulting in more reactive/accessible structures towards the hydrolysis of cellulose.

3.2. Influence of enzymatic hydrolysis time on CNC yield

Overall, cellulose is composed of long, unbranched chains of β-1,4-linked glucose units, held together in the microfibril through hydrogen bonds and Van der Waals forces, forming a crystalline, organized structure that is refractory to hydrolysis in certain areas of the microfibril (Pérez, Munoz-Dorado, de la Rubia, & Martinez, 2002). Highly ordered, crystalline regions are interspersed with regions containing disorganized or amorphous cellulose, which

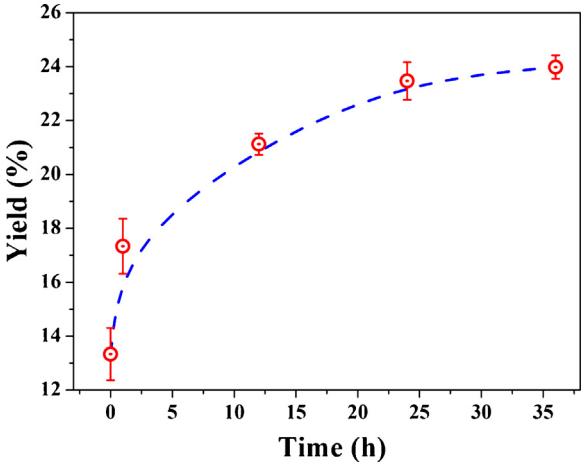

Fig. 1. Effect of enzymatic hydrolysis time on CNC yield.

constitute 5–20% of the microfibril. Amorphous regions are more susceptible to enzymatic degradation (Abdul Khalil, Bhat, & Ireana Yusra, 2012; Tibolla et al., 2014), and the endoglucanase enzyme to selectively hydrolyze the amorphous region while leaving the crystalline region has been developed (Filson et al., 2009). In this regard, the applied enzymatic hydrolysis would offer the potential for high yields, high selectivity, low energy costs and mild operating conditions in the extraction of CNC from OCC. Herein, the role of enzymatic hydrolysis of the combined process in the elevation of CNC yield from OCC pulp fiber was investigated, and the results are shown in Fig. 1.

As shown in Fig. 1, the CNC yield was 13.3% in the absence of enzymatic treatment; whereas, a pronounced change in CNC yield might be expected in the presence of enzymatic treatment. Specifically, when the mixture after phosphoric acid hydrolysis was further subjected to enzymatic treatment for 1 h, followed by sonication, the final CNC yield reached 17.33%. This efficiency was in consistent with the results reported in a previous study (Filson et al., 2009) where the CNC yield was increased 4.03% as a function of enzymatic treatment for 1 h. Additionally, when further increasing the enzymatic hydrolysis time to 12, 24 and 36 h, the CNC yield changed to 21.12, 23.47 and 23.98%, respectively. It could be noted that CNC yield showed a slight uptrend when the enzymatic hydrolysis time was over 24 h under the condition studied. Similar results regarding the CNC yield as a function of enzymatic hydrolysis time had ever been reported in the literature (Ma, Zhang, Cao, & Yao, 2014).

3.3. TEM observations

Typical TEM images of CNC samples produced from acid hydrolysis/enzymatic hydrolysis (24 h)/sonication process are demonstrated in Fig. 2. It can be seen that the CNC sample exhibited a rod-like structure with a length of 100–400 nm and a width of 15–80 nm, similar to the observation reported in the previous work (Wang, Sain, & Oksman, 2007).

3.4. Particle size distribution of CNC samples

The particle size distribution and average particle size of each CNC sample are depicted in Fig. 3. It is evident that enzymatic hydrolysis exerted an important role in the particle size distribution of CNC samples. Without enzymatic treatment, the CNC sample showed an overall particle size range of 300–6000 nm, and had an average particle size of 1752 nm, presumably due to the serious aggregation of the obtained CNC particles in water (Cheng et al., 2015). However, subjected to enzymatic treatment, the CNC sample exhibited a marked decrease in particle size range and average particle size. Specifically, the CNC sample enzymatically treated for 24 h showed the particle size distribution of 100–500 and 1350–3850 nm, with an average particle size of 401 nm, very close to the previously reported results (Fan & Li, 2012). Furthermore, increasing the enzymatic hydrolysis time, the particle size of the obtained CNC sample was pronouncedly decreased. The decreased particle size of CNC as a function of the applied enzymatic treatment would facilitate the reinforcement effect of CNC in related composites.

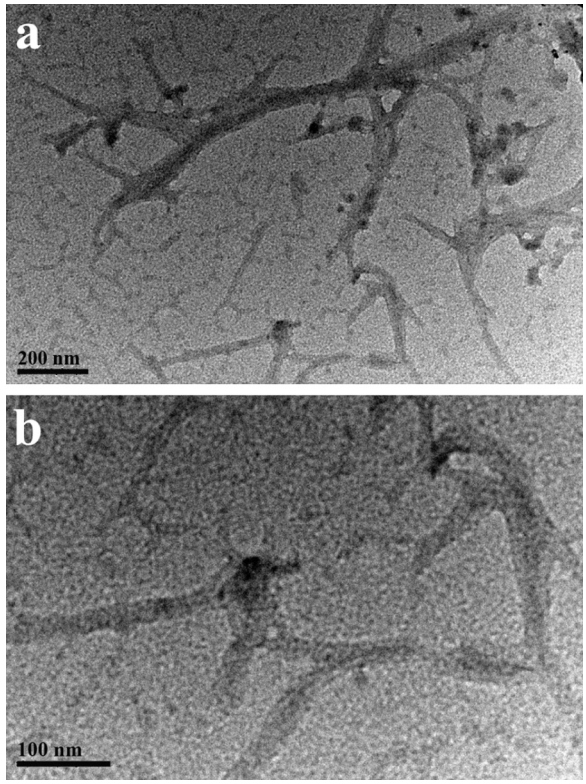

Fig. 2. TEM images (with different magnification) of CNC samples produced from acid hydrolysis/enzymatic hydrolysis (24 h)/sonication process.

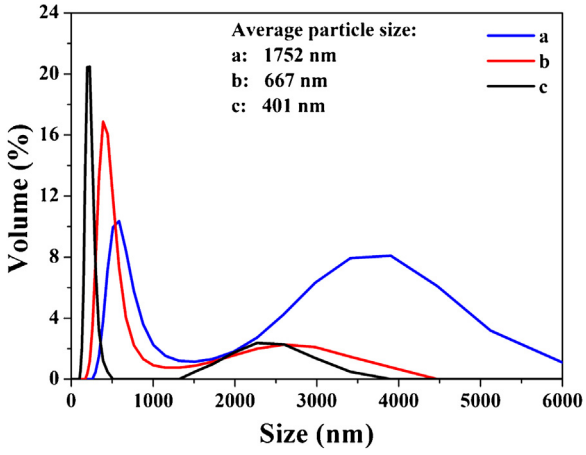

Fig. 3. Particle size distribution and average particle size of CNC samples produced from (a) acid hydrolysis/sonication process, (b) acid hydrolysis/enzymatic hydrolysis (1 h)/sonication process, and (c) acid hydrolysis/enzymatic hydrolysis (24 h)/sonication process.

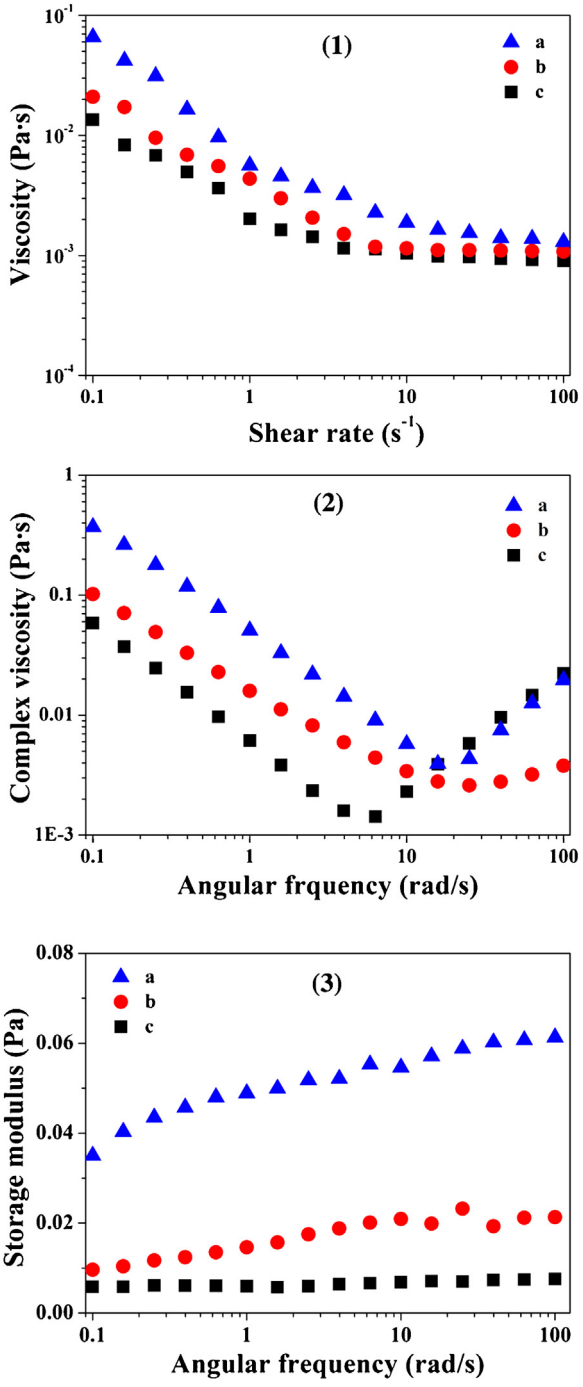

Fig. 4. (1) Viscosity as a function of shear rate, (2) complex viscosity as a function of angular frequency, and (3) storage modulus as a function of angular frequency for CNC samples produced from (a) acid hydrolysis/sonication process, (b) acid hydrolysis/enzymatic hydrolysis (1 h)/sonication process, and (c) acid hydrolysis/enzymatic hydrolysis (24 h)/sonication process.

3.5. Rheological behavior of CNC suspensions

Rheological measurement is a well-known method for evaluating the structure information of bio-polymer suspensions (Loret, Meunier, Frith, & Fryer, 2004). The shear viscosity curves of CNC suspensions as a function of shear rate and production processes are shown in Fig. 4(1). It can be observed that all CNC suspensions exhibited a visible shear-thinning behavior. However, in comparison with the CNC sample without enzymatic treatment, the CNC sample produced from the combined process displayed a pronounced decrease in viscosity, which may be due to the progressive removal of amorphous area of cellulose structure leading to the decreased degree of polymerization (Han, Lei, & Wu, 2014; Le Goff, Gaillard, Helbert, Garnier, & Aubry, 2014). In addition, the complex viscosity of CNC suspensions as a function of angular frequency was investigated, and the result is shown in Fig. 4(2). As a whole, the complex viscosity curves of all samples showed two distinct regions. At a lower frequency, the complex viscosity decreased with the increased frequency. At a higher frequency, a transition was observed and the complex viscosity increased with the increased frequency. Specifically, the turning point of CNC (a), (b) and (c) occurred at 15.8, 25.1 and 6.31, respectively. Viscoelastic curves of CNC suspensions are presented in Fig. 4(3). As the angular frequency increased, the storage modulus of CNC suspensions increased, although this increase was less evident with the increased enzymatic hydrolysis time. This result indicated a gel-like behavior due to the high aspect ratio of the nanofibril gelation network (Liu, Chen, Yue, Chen, & Wu, 2011).

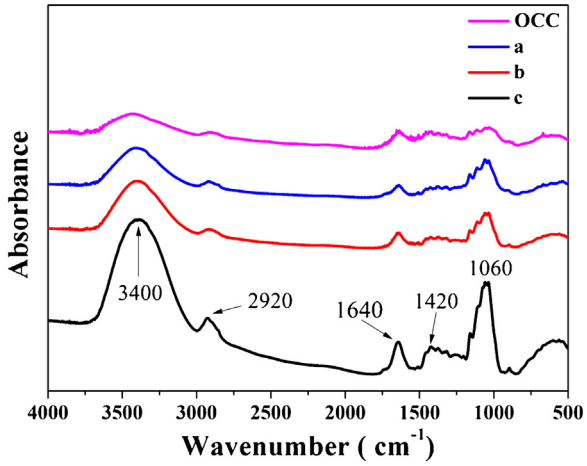

Fig. 5. FT-IR spectra of OCC and CNC samples produced from (a) acid hydrolysis/sonication process, (b) acid hydrolysis/enzymatic hydrolysis (1 h)/sonication process, and (c) acid hydrolysis/enzymatic hydrolysis (24 h)/sonication process.

3.6. FT-IR spectra analysis

FT-IR spectra of OCC and CNC samples obtained from different processes are shown in Fig. 5. Overall, the FT-IR absorbance peaks of OCC and CNC samples were similar. Specifically, the broad absorption band at 3400 cm^{-1} was due to the —OH stretching vibrations. The absorption peaks at 2920 cm^{-1} and 1420 cm^{-1} mainly corresponded to symmetric and asymmetric —CH stretching vibrations (Kolmas, Oledzka, Sobczak, & Nałęcz-Jawecki, 2014). The absorption bands at 1640 cm^{-1} and 1170 cm^{-1} were probably associated with the C=O and C—O stretching motions (Rosa et al., 2010). These main absorption peaks greatly supported the cellulose structure of all samples. In comparison with OCC sample, there were marked increases in the absorption intensity at the corresponding bands for CNC samples. This characteristic was more evident for the CNC sample derived from acid hydrolysis/enzymatic hydrolysis (24 h)/sonication process. Similar results were reported in the previous work (Khan et al., 2012). The increased absorption intensity may be considered to be related to the increased crystallinity (O'Connor, DuPré, & Mitcham, 1958).

3.7. X-ray Diffraction analysis

X-ray diffraction patterns of all CNC samples are shown in Fig. 6. As a whole, the main peaks of all samples appeared at 15.7, 22.8

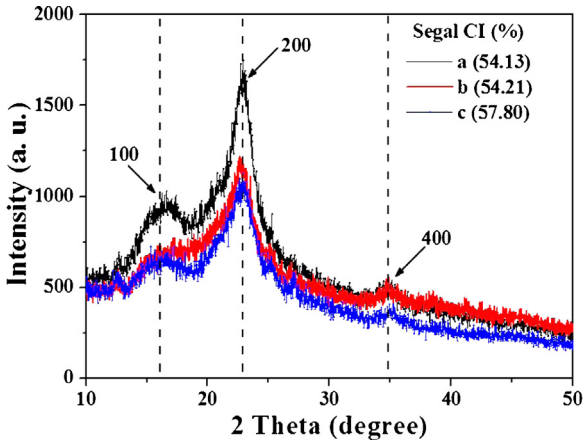

Fig. 6. X-ray diffraction patterns of CNC samples produced from (a) acid hydrolysis/sonication process, (b) acid hydrolysis/enzymatic hydrolysis (1 h)/sonication process, and (c) acid hydrolysis/enzymatic hydrolysis (24 h)/sonication process.

and 34.1°, attributed to the diffraction planes of (1 1 0), (2 0 0) and (4 0 0), respectively, all of which represented the characteristic diffraction peaks of cellulose I (Mansikkamäki, Lahtinen, & Rissanen, 2007). This result suggested that both phosphoric acid hydrolysis and enzymatic hydrolysis had a limited effect on the polymorphism of cellulose I for the CNC sample produced.

Moreover, X-ray diffraction patterns reflected an increase in the crystalline domains in the CNC as a function of the use of enzymatic hydrolysis (Fig. 6). This was evidenced by the presence of the significantly increased intensity of diffraction peaks at 15.7° and 22.8°. The intensity of diffraction peaks at 15.7° and 22.8° were ascribed to the content of cellulose I (native cellulose). To further understand the crystal structure, the Segal CI of CNC samples were calculated and presented in Fig. 6. It was shown that enzymatic hydrolysis process increased the crystallinity of the resultant CNC samples. The improved crystallinity as a result of enzymatic hydrolysis may be due to the amorphous phase removed by cellulase. Similar results were reported in the literature (Pääkkö et al., 2007). In contrast, the Segal CI of the CNC samples was lower than that reported in previous studies (Chen et al., 2011; Tang et al., 2014). This result may be due to the fact that mechanical and chemical treatments of pulp in the recycling process increase the amorphous regions and reduce the cellulose chain length of cellulose molecules, cumulatively decreasing the crystallinity of the resultant product (Filson et al., 2009).

3.8. Thermal decomposition analysis

TG and DTG curves of OCC and CNC samples are demonstrated in Fig. 7(1) and (2), respectively. As can be seen, in low temperature (<100 °C) range, all samples exhibited a similar weight loss because of the evaporation of absorbed water. In high temperature range, the weight loss of all samples was different with each other. The OCC sample had higher thermal stability than CNC samples, and the pronounced decomposition onset was at 300 °C, the temperature of the maximum decomposition rate was 365 °C; decomposition was complete at 400 °C. For CNC samples, different production processes conferred different thermal decomposition behavior to each sample, as clearly shown in DTG curves (Fig. 7(2)). The temperature of the maximum decomposition rate for CNC (a), (b) and (c) was at 276, 284 and 312 °C, respectively, providing direct evidence that the thermal stability of CNC samples was increased with the increased enzymatic hydrolysis time. Furthermore, the CNC samples obtained here exhibited better thermal stability in comparison to that derived from sulfuric acid hydrolysis process as reported in the literature (Liu et al., 2014; Tang et al., 2014). This result would be advantageous for the potential application of CNC in related polymer-based composites. In addition, the amounts of the char residues for OCC, CNC (a), (b) and (c) were 19.03, 18.88, 13.84, and 4.90%, respectively (Fig. 7(1)). The decreased char residue for CNC samples may be largely related to the increased split hydrogen bonds (Fattahi Meyabadi, Dadashian, Mir Mohamad Sadeghi, & Ebrahimi Zanjani Asl, 2014).

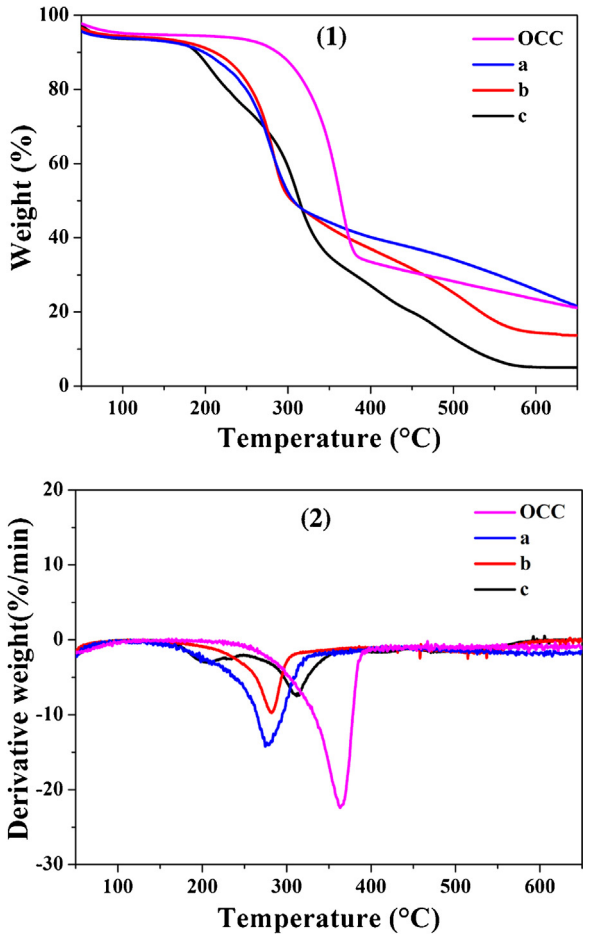

Fig. 7. (1) TG-curves, (2) DTG-curves of OCC and CNC samples produced from (a) acid hydrolysis/sonication process, (b) acid hydrolysis/enzymatic hydrolysis (1 h)/sonication process, and (c) acid hydrolysis/enzymatic hydrolysis (24 h)/sonication process.

4. Conclusions

The concept of using a combined process (*i.e.*, acid hydrolysis/enzymatic hydrolysis/sonication) to produce CNC from low-cost OCC material was developed/demonstrated. Results showed that the applied enzymatic hydrolysis was effective in enhancing the CNC yield after phosphoric acid hydrolysis. In the absence of enzymatic treatment, the CNC yield was 13.3%; while the enzymatic treatment for 1, 12, 24 and 36 h made the CNC yield increased by 17.33, 21.12, 23.47 and 23.98%, respectively, which would greatly facilitate the economics of the industrial CNC production. Furthermore, it was shown that the CNC sample exhibited a rod-like structure with a length of 100–400 nm and a width of 15–80 nm and displayed the crystal form of cellulose I. In addition, the enzymatic treatment led to the increased crystallinity and thermal stability of CNC.

Acknowledgements

This work was financially supported by the National Natural Science Foundation of China (grant no. 31100442), Zhejiang Provincial Natural Science Foundation of China (grant no. LY14C160003), Zhejiang Provincial Top Key Academic Discipline of Chemical Engineering, Technology, Zhejiang Open Foundation of the Most Important Subjects (grant no. 2014YXQN01), 521 Talent Cultivation Program of Zhejiang Sci-Tech University (grant no. 11110132521310) and Open Foundation of the Key Lab of Pulp and Paper Science & Technology of Ministry of Education, Qilu University of Technology (grant no. 201403).

References

Abdul Khalil, H. P. S., Bhat, A. H., & Ireana Yusra, A. F. (2012). Green composites from sustainable cellulose nanofibrils: A review. *Carbohydrate Polymers*, *87*(2), 963–979.

Bai, W., Holbery, J., & Li, K. (2009). A technique for production of nanocrystalline cellulose with a narrow size distribution. *Cellulose*, *16*(3), 455–465.

Beck-Candanedo, S., Roman, M., & Gray, D. G. (2005). Effect of reaction conditions on the properties and behavior of wood cellulose nanocrystal suspensions. *Biomacromolecules*, *6*(2), 1048–1054.

Brinchi, L., Cotana, F., Fortunati, E., & Kenny, J. M. (2013). Production of nanocrystalline cellulose from lignocellulosic biomass: Technology and applications. *Carbohydrate Polymers*, *94*(1), 154–169.

Camarero Espinosa, S., Kuhnt, T., Foster, E. J., & Weder, C. (2013). Isolation of thermally stable cellulose nanocrystals by phosphoric acid hydrolysis. *Biomacromolecules*, *14*(4), 1223–1230.

Cha, R., He, Z., & Ni, Y. (2012). Preparation and characterization of thermal/pH-sensitive hydrogel from carboxylated nanocrystalline cellulose. *Carbohydrate Polymers*, *88*(2), 713–718.

Chen, W., Yu, H., Liu, Y., Chen, P., Zhang, M., & Hai, Y. (2011). Individualization of cellulose nanofibers from wood using high-intensity ultrasonication combined with chemical pretreatments. *Carbohydrate Polymers*, *83*(4), 1804–1811.

Cheng, D., Wen, Y., Wang, L., An, X., Zhu, X., & Ni, Y. (2015). Adsorption of polyethylene glycol (PEG) onto cellulose nano-crystals to improve its dispersity. *Carbohydrate Polymers*, *123*(5), 157–163.

de Campos, A., Correa, A. C., Cannella, D., Teixeira, E. d. M., Marconcini, J. M., Dufresne, A., et al. (2013). Obtaining nanofibers from curaua and sugarcane bagasse fibers using enzymatic hydrolysis followed by sonication. *Cellulose*, *20*(3), 1491–1500.

Engström, A. C., Ek, M., & Henriksson, G. (2006). Improved accessibility and reactivity of dissolving pulp for the viscose process: Pretreatment with monocomponent endoglucanase. *Biomacromolecules*, *7*(6), 2027–2031.

Fan, J. S., & Li, Y. H. (2012). Maximizing the yield of nanocrystalline cellulose from cotton pulp fiber. *Carbohydrate Polymers*, *88*(4), 1184–1188.

Fattahi Meyabadi, T., Dadashian, F., Mir Mohamad Sadeghi, G., & Ebrahimi Zanjani Asl, H. (2014). Spherical cellulose nanoparticles preparation from waste cotton using a green method. *Powder Technology*, *261*, 232–240.

Filson, P. B., & Dawson-Andoh, B. E. (2009). Sono-chemical preparation of cellulose nanocrystals from lignocellulose derived materials. *Bioresource Technology*, *100*(7), 2259–2264.

Filson, P. B., Dawson-Andoh, B. E., & Schwegler-Berry, D. (2009). Enzymatic-mediated production of cellulose nanocrystals from recycled pulp. *Green Chemistry*, *11*(11), 1808–1814.

Flauzino Neto, W. P., Silvério, H. A., Dantas, N. O., & Pasquini, D. (2013). Extraction and characterization of cellulose nanocrystals from agro-industrial residue – Soy hulls. *Industrial Crops and Products*, *42*, 480–488.

French, A. D., & Cintrón, M. S. (2013). Cellulose polymorphy, crystallite size, and the Segal crystallinity index. *Cellulose*, *20*(1), 583–588.

Guo, W. J., Wang, Y., Wan, J. Q., & Ma, Y. W. (2011). Effects of slushing process on the pore structure and crystallinity in old corrugated container cellulose fibre. *Carbohydrate Polymers*, *83*(1), 1–7.

Han, J., Lei, T., & Wu, Q. (2014). High-water-content mouldable polyvinyl alcohol-borax hydrogels reinforced by well-dispersed cellulose nanoparticles: Dynamic rheological properties and hydrogel formation mechanism. *Carbohydrate Polymers*, *102*, 306–316.

Hunter, F. R., & Park, D. W. (1998). Method of enhancing strength of paper products and the resulting products, U.S. Patent.

Khan, A., Khan, R. A., Salmieri, S., Le Tien, C., Riedl, B., Bouchard, J., et al. (2012). Mechanical and barrier properties of nanocrystalline cellulose reinforced chitosan based nanocomposite films. *Carbohydrate Polymers*, *90*(4), 1601–1608.

Kolmas, J., Oledzka, E., Sobczak, M., & Nałęcz-Jawecki, G. (2014). Nanocrystalline hydroxyapatite doped with selenium oxyanions: A new material for potential biomedical applications. *Materials Science and Engineering C*, *39*, 134–142.

Le Goff, K. J., Gaillard, C., Helbert, W., Garnier, C., & Aubry, T. (2014). Rheological study of reinforcement of agarose hydrogels by cellulose nanowhiskers. *Carbohydrate Polymers*, *116*, 117–123.

Li, S., Li, C., Li, C., Yan, M., Wu, Y., Cao, J., et al. (2013). Fabrication of nano-crystalline cellulose with phosphoric acid and its full application in a modified polyurethane foam. *Polymer Degradation and Stability*, *98*(9), 1940–1944.

Li, W., Wang, R., & Liu, S. (2011). Nanocrystalline cellulose prepared from soft-wood kraft pulp via ultrasonic-assisted acid hydrolysis. *BioResources*, *6*(4), 4271–4281.

Li, W., Yue, J., & Liu, S. (2012). Preparation of nanocrystalline cellulose via ultrasound and its reinforcement capability for poly (vinyl alcohol) composites. *Ultrasonics Sonochemistry*, *19*(3), 479–485.

Li, Y., Li, G., Zou, Y., Zhou, Q., & Lian, X. (2014). Preparation and characterization of cellulose nanofibers from partly mercerized cotton by mixed acid hydrolysis. *Cellulose*, *21*(1), 301–309.

Liu, D. G., Chen, X. Y., Yue, Y. Y., Chen, M. D., & Wu, Q. L. (2011). Structure and rheology of nanocrystalline cellulose. *Carbohydrate Polymers*, *84*(1), 316–322.

Liu, Y., Wang, H., Yu, G., Yu, Q., Li, B., & Mu, X. (2014). A novel approach for the preparation of nanocrystalline cellulose by using phosphotungstic acid. *Carbohydrate Polymers*, *110*, 415–422.

Loret, C., Meunier, V., Frith, W. J., & Fryer, P. J. (2004). Rheological characterisation of the gelation behaviour of maltodextrin aqueous solutions. *Carbohydrate Polymers*, *57*(2), 153–163.

Lu, H., Gui, Y., Zheng, L., & Liu, X. (2013). Morphological, crystalline, thermal and physicochemical properties of cellulose nanocrystals obtained from sweet potato residue. *Food Research International*, *50*(1), 121–128.

Ma, L., Zhang, Y., Cao, J., & Yao, J. (2014). Preparation of unmodified cellulose nanocrystals from phyllostachys heterocycla and their biocompatibility evaluation. *Bioresources*, *9*(1), 210–217.

Mansikkamäki, P., Lahtinen, M., & Rissanen, K. (2007). The conversion from cellulose I to cellulose II in NaOH mercerization performed in alcohol–water systems: An X-ray powder diffraction study. *Carbohydrate Polymers*, *68*(1), 35–43.

Nguyen, X., Shariff, A., Earl, P., & Eamer, R. (1993). Bleached pulps for printing and writing papers from old corrugated containers. *Progress in Paper Recycling*, *3*(2), 25–32.

O'Connor, R. T., DuPré, E. F., & Mitcham, D. (1958). Applications of infrared absorption spectroscopy to investigations of cotton and modified cottons. Part I: Physical and crystalline modifications and oxidation. *Textile Research Journal*, *28*(5), 382–392.

Pääkkö, M., Ankerfors, M., Kosonen, H., Nykänen, A., Ahola, S., Österberg, M., et al. (2007). Enzymatic hydrolysis combined with mechanical shearing and high-pressure homogenization for nanoscale cellulose fibrils and strong gels. *Biomacromolecules*, *8*(6), 1934–1941.

Pérez, J., Munoz-Dorado, J., de la Rubia, T., & Martinez, J. (2002). Biodegradation and biological treatments of cellulose, hemicellulose and lignin: An overview. *International Microbiology*, *5*(2), 53–63.

Pirani, S., & Hashaikeh, R. (2013). Nanocrystalline cellulose extraction process and utilization of the byproduct for biofuels production. *Carbohydrate Polymers*, *93*(1), 357–363.

Rosa, M., Medeiros, E., Malmonge, J., Gregorski, K., Wood, D., Mattoso, L., et al. (2010). Cellulose nanowhiskers from coconut husk fibers: Effect of preparation conditions on their thermal and morphological behavior. *Carbohydrate Polymers*, *81*(1), 83–92.

Sun, B., Hou, Q., He, Z., Liu, Z., & Ni, Y. (2014). Cellulose nanocrystals (CNC) as carriers for a spirooxazine dye and its effect on photochromic efficiency. *Carbohydrate Polymers*, *111*, 419–424.

Tang, Y., Yang, S., Zhang, N., & Zhang, J. (2014). Preparation and characterization of nanocrystalline cellulose via low-intensity ultrasonic-assisted sulfuric acid hydrolysis. *Cellulose*, *21*(1), 335–346.

Tibolla, H., Pelissari, F. M., & Menegalli, F. C. (2014). Cellulose nanofibers produced from banana peel by chemical and enzymatic treatment. *LWT – Food Science and Technology*, *59*(2), 1311–1318.

Tischer, P. C. S. F., Sierakowski, M. R., Westfahl, H., & Tischer, C. A. (2010). Nanostructural reorganization of bacterial cellulose by ultrasonic treatment. *Biomacromolecules*, *11*(5), 1217–1224.

Wan, J., Yang, J., Ma, Y., & Wang, Y. (2011). Effects of the pulp preparation and papermaking processes on the properties of OCC fibers. *BioResources*, *6*(2), 1615–1630.

Wang, B., Sain, M., & Oksman, K. (2007). Study of structural morphology of hemp fiber from the micro to the nanoscale. *Applied Composite Materials*, *14*(2), 89–103.

Xiong, R., Zhang, X., Tian, D., Zhou, Z., & Lu, C. (2012). Comparing microcrystalline with spherical nanocrystalline cellulose from waste cotton fabrics. *Cellulose*, *19*(4), 1189–1198.

Xu, Y., Salmi, J., Kloser, E., Perrin, F., Grosse, S., Denault, J., et al. (2013). Feasibility of nanocrystalline cellulose production by endoglucanase treatment of natural bast fibers. *Industrial Crops and Products*, *51*, 381–384.

Yu, H., Qin, Z., Liang, B., Liu, N., Zhou, Z., & Chen, L. (2013). Facile extraction of thermally stable cellulose nanocrystals with a high yield of 93% through hydrochloric acid hydrolysis under hydrothermal conditions. *Journal of Materials Chemistry A*, *1*(12), 3938–3944.

Zaman, M., Liu, H., Xiao, H., Chibante, F., & Ni, Y. (2013). Hydrophilic modification of polyester fabric by applying nanocrystalline cellulose containing surface finish. *Carbohydrate Polymers*, *91*(2), 560–567.